Indian Journal of Chemical Technology
Vol. 26, November, 2019 pp. 522-528

Dip coating of forsterite-hydroxyapatitie-poly (ε-caprolactone) nanocomposites on Ti6Al4Vsubstrates for its corrosion prevention

Shivendra Kumar[1], P Shakti Prakash[*,1], Surendra Kumar Barnwal[1], Suryappa Jayappa Pawar[1], Ravi Prakash Tewari[1], Gopal Ji[2] & Rajiv Prakash[2]

[1]Department of Applied Mechanics, Motilal Nehru National Institute of Technology Allahabad, Prayagraj 211 004, Uttar Pradesh, India.
[2]School of Materials Science and Technology, Indian Institute of Technology (BHU), Varanasi 221 003, Uttar Pradesh, India.

E-mail: pspsbme@gmail.com

Received 14 April 2019; accepted 16 October 2019

Titanium and titanium alloys are extensively used in biomedical, cardiac and cardiovascular applications for their superb properties, such as good fatigue strength, low modulus, machinability, formability, corrosion resistance and biocompatibility. However, titanium and its alloys do not meet the majority of all clinical necessities. Due to these reasons, surface modification is frequently performed to enhance the mechanical, biological and chemical properties of titanium and alloys. In this work, nanocomposites coating of poly(ε-caprolactone)/hydroxyapatite/forsterite (PCL/HA/F) have been successfully deposited on the Ti6Al4V substratesby dip coating at room temperature. The coatings are prepared with various concentrations of forsterite/hydroxyapatite nanopowder (2, 4, 6 and 8 wt.%) with a fixed concentration of PCL (4 wt.%) and thus coated Ti6Al4V substrates are examined for corrosion resistance. PCL/Hydroxyapatite/Forsterite coatings are characterized by X-ray diffraction (XRD) and scanning electron microscopy (SEM), which clearly showed the formation of nanocomposites. Potentiodynamic polarization curves and electrochemical impedance spectroscopy (EIS) are used to investigate corrosion behavior of the coated substrates, which portrayed that the composite coating of PCL/HA/F substantially enhanced the corrosion resistance of Ti6Al4V alloy.

Keywords: Corrosion, Forsterite, Hydroxyapatite, Nanocomposite, Poly(ε-caprolactone), Ti6Al4V

Increase in use of metals and their alloys in the field of biomedical field (like orthopedic implants) shows their wide acceptability as biomaterials. The most essential properties required by biomaterial under load-bearing applications are toughness and mechanical strength. Some of the metals like stainless steels, Co-Cr compounds, industrially pure titanium (CP-Ti) and its alloys are generally used as biomaterials for their superb mechanical properties[1]. Among the metals used as implants, titanium and titanium alloys have demonstrated good biocompatibility and osseointegration with various metals[2]. Titanium and Ti-alloys used in the biomedical application have excellent characteristics of low density, good strength, corrosion resistance and biocompatibility, which impart them uniqueness among all metallic materials. Commercially pure titanium (CP-Ti) and Ti6Al4V alloys have been one of the first titanium materials utilized for biomedical applications. Even today, they are used as bio-materials on a large scale. So, titanium and its alloys have been always the best choice for biomedical applications, particularly as hard tissue replacement as well as in cardiac and cardiovascular applications. The reasons are low modulus, good fatigue strength, formability, good machinability, high corrosion resistance and excellent biocompatibility of Ti and Ti-alloys[3].

Titanium implants used in the human body get oxidized and may have stressed, plastically distorted and non-uniform surface layer, which can actuate the issues like wear and corrosion. Such local surfaces are not appropriate for biomedical applications and some surface treatment must be performed[4]. The most ideal surface change procedures not only hold the amazing bulk properties of titanium and its alloys but also improve specific surface properties required by different clinical applications[5]. Various researches have focused on different ways to deal with improvement in corrosion resistance of titanium and its alloys in the biological environment. But surface treatment with various surface alteration techniques and coatings with various bioactive ceramics, polymers and composites have been one of the best

convincing strategies to increase biocompatibility, corrosion resistant and osseointegration of titanium and its alloys[6].

Compared to pure ceramic coatings, composite coatings are proved more effective in reduction of brittleness and crack formation, which has provided improved corrosion resistance[7]. Hydroxyapatite [HA, $Ca_{10}(PO_4)_6(OH)_2$] has shown promising characteristics amongst the most vital individual from calcium phosphate aggregate. The mineralogical composition of HA resembles to natural bone[8] and therefore it is suitable for bone substitution and reconstruction[9]. Moreover, HA has demonstrated significant accomplishment in implants because of its positive *in-vivo* behavior[10,11]. It is also proved thatthe presence of HA films prolongs the lifetime of prostheses[12]. Besides good compatibility with human body and properties, its brittleness and weak mechanical properties restrict its direct use in load-bearing applications. To be utilized viably in such applications, the mechanical properties of HA should be improved. The incorporation of other ceramics with better mechanical properties may enhance the mechanical properties of HA[13]. Forsterite (F, Mg_2SiO_4) is a member ofthe olivine family. It has an orthorhombic crystalline structure, high surface area and extraordinary chemical stability. Owing to its superb bioactivity, biocompatibility, and favored mechanical properties over calcium phosphates, forsterite has been widely examined for its applications in bone repair and tissue building[14]. Now a day, polymeric-ceramic composite coatings are preferred to obtain a crack-free and dense packed coating on substrates. Different kinds of polymers have been applied as coatings for biomedical applications, such aspoly(l-lactic acid) (PLLA), poly(ε-caprolactone) (PCL) and poly (glycolic acid) (PGA)[15]. PCL is a semi-crystalline aliphatic polymer with incredible biocompatibility, sustained biodegradability and superb mechanical properties[16]. PCL is alluring due to its low cost, sustained biodegradability,and low atomic weight. Contrasted to other biodegradable polymers, PCL exhibits better mechanical properties. So, itmakes it sensible to use PCL for load-bearing applications[15]. Since we stated in the above paragraph that composites coatings are more successful than the alone polymer or alone ceramic coatings, PCL/HA/F composite coatings are used for examination in this work.

The primary aim of this work is to deposit PCL/HA/F composite coatings on Ti6Al4V and to investigate its corrosion behaviour. The composite coatings are prepared with different concentration of HA and forsterite nanopowder dispersed infixed concentration of PCL and coated on Ti6Al4V substrates by dip coating. Dip coating is selected to coat the substrates because it is an easy and effective method[17]. Thus, coated Ti6Al4V substrates are examined for adhesion and corrosion tests. The corrosion tests include potentio-dynamic polarization test (PPT) and electrochemical impedance spectroscopy (EIS). The results show that PCL/HA/F composite coatings increase corrosion resistance and biocompatibility of Ti6Al4V substrates.

Experimental Section

Synthesis of forsterite nanopowder

Fosterite nanopowder were synthesized using magnesium nitrate hexahydrate [Mg(NO3)$_2$. 6H2O(MNH), Merck, 99.99% purity], colloidal silica (SiO_2, 34 wt.% solid fraction, Sigma), sucrose (Merck, 99.9% purity), and polyvinyl Alcohol (PVA, Merck, molecular weight = 72,000). Initially, magnesium nitrate hexahydrate (MNH) was dissolved in distilled water and colloidal silica (34 wt.%) was added during stirring. Afterward, the sucrose solution was prepared by adding sucrose in distilled water. PVA solution was prepared by adding PVAin distilled water and put on stirring at 50°C for 30 min. Finally, all solutions were mixed and the *p*H of the solution was adjusted to *p*H=1 using nitric acid (Merck). Then, the solution was vigorously stirred at 80°C to promote gelation. After the gel formation, the gel was dried at 200°C in a hot air oven and grounded in a mortar manually to make fine powders. To remove residual volatiles, the powder was calcined at 1000°C in a mufflefurnace. The calcined powder was re-grounded in a mortarby pestle to get forsterite nanopowder. For a clear understanding, the schematic of the synthesis process is shown in Fig. 1.

Preparation of Ti6Al4V substrates

The substrates were of size 10 mm × 10 mm and obtained by cutting hot rolled titanium sheet (thickness-3mm) by WIRE EDM process. Prior to the start coating process, the substrates were mirror-polished by rubbing it on different grit-sized SiC papers (400 to 2000) followed by rinsing with soap and washing with double distilled water. Then after, the substrates were ultrasonicated for 15 min by using

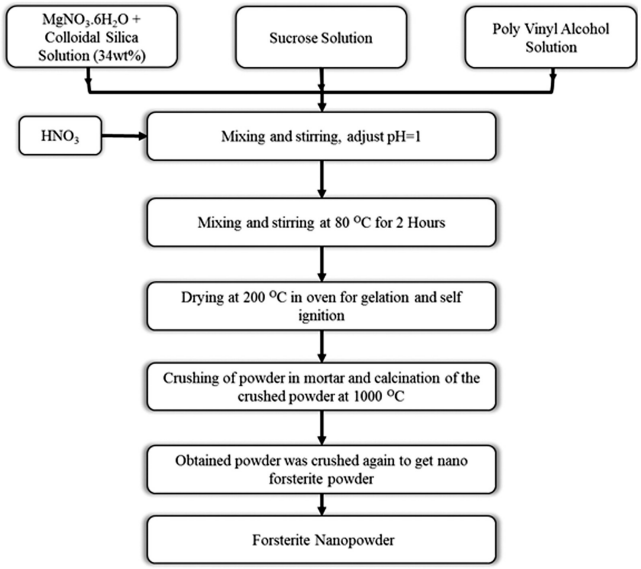

Fig. 1 — Schematic flow chart for the synthesis of forsterite nano-powder.

deionized water and ethanol. In this way, the mirror polished substrates were prepared for deposition.

Preparation of PCL/HA/Forsterite slurry

Initially, Poly(e-caprolactone) solution was prepared by dissolving the PCL pellets (Sigma Aldrich, UK, Mw=80000) in chloroform at room temperature and stirred it continuously till clear 4 wt. % PCL solution was formed. Then, forsterite and hydroxyapatite nanopowder were added to PCL solution in different concentrations (2, 4, 6 and 8 wt. %) to form the suspension.The suspensions were agitated at room temperature for 24 h to produce homogeneously dispersed HA/Forsterite nanopowder in PCL solution.

Deposition of PCL/HA/forsterite composite onto Ti6Al4V

Thin film of composites on Ti6Al4V substrates was deposited by dipping them in to the suspension of PCL/HA/F with the help of dip coater. Substrates were dipped into suspensions for 2 min with dipping speed of 50 mm/min, withdrawn at fixed speed of 100 mm/min, dried at room temperature for 2 min and dipped again in the suspension to coat more layers. After the whole process, the coated substrates were dried in an oven at 60°C for 12 h.

Characterization of the nanocomposite coated substrates

The phase compositions of forsterite powder, HA powder, Ti6Al4V substrate and PCL/HA/F nanocomposite coating were analyzed by RIGAKU smart lab X-Ray diffractometer. The details were as follows: operating temperature, 40 kV; operating current, 40 mA; and with CuKα radiation, λ =1.540 Å. The XRD patterns were recorded inthe 2θ range of 20–90˚, with a step size of 0.02˚ and a step time of 1 s. The crystallite size of the HA powder was calculated using Scherrer's formula[18]

$$t= 0.9\lambda/\beta \cos\theta \quad \ldots (1)$$

where t is the size of the crystal, λ is the wavelength of the radiation β is the full width at half maxima and θ is the position of the maxima of diffraction.

Characteristic functional groups of forsterite, HA and PCL/HA/Forsterite nano-composites were identified by analyzing material mixed KBr pallets using Nicolet iS5, FTIR spectrometer. FTIR spectra were recorded in the region of 400–4000 cm^{-1} with a scan rate of 4 cm^{-1},averaging over 128 scans.

The surface morphology of the coated Ti6Al4V substrates was examined by FEI, Nova Nano SEM. Prior to SEM analysis, all the samples were sputter coated with gold to prevent electrostatic charging.

Potentiodynamic polarization curves and EIS were utilized for measuring the corrosion behavior of the uncoated and coated titanium alloy (Ti6Al4V) substrates in standard buffer phosphate saline (PBS). Three electrodes set up (silver/silver chloride, platinum foil, and sample) was used for the electrochemical tests. The electrodes were given their usual voltages. The effective area of the working electrode in each case was 0.5 cm^2. Polarization test was performed in the potential range OCP±300 mV at a scanning speed of 1 mV per second. For EIS, AC signal of 10 mV was scanned in range was 10^5 Hz -10^{-3} Hz at OCP. Protection efficiencies ($\eta_{Rp}$and η_{Rct}) were calculated based on corrosion current density (i_{corr}) and charge transfer resistance (R_{ct}) by the equations[19]:

$$\eta_{Rp}(\%) = \frac{I^o_{corr} - I^i_{corr}}{I^o_{\mathrm{corr}}} \times 100 \quad \ldots (2)$$

where ^{o} *and* ^{i} superscripts denote readings in blank solution and inhibited solution.

Results and Discussion

XRD analysis of forsterite and hydroxyapatite nanopowder

The X-ray diffraction of as-synthesized forsterite nanopowder is shown in Fig. 2. The four strongest XRD peaks for forsterite were detected with Miller indices (121), (311), (221) and (210), which corresponded to Bragg angles 36.504, 35.702, 39.075

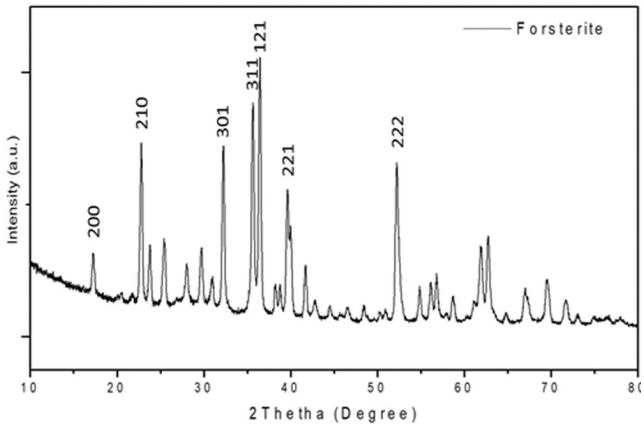

Fig. 2 — XRD pattern of synthesized forsterite nanopowder.

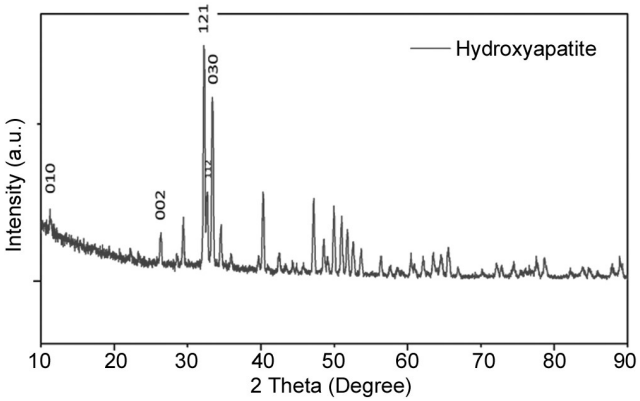

Fig. 3 — XRD pattern of hydroxyapatite nanopowder.

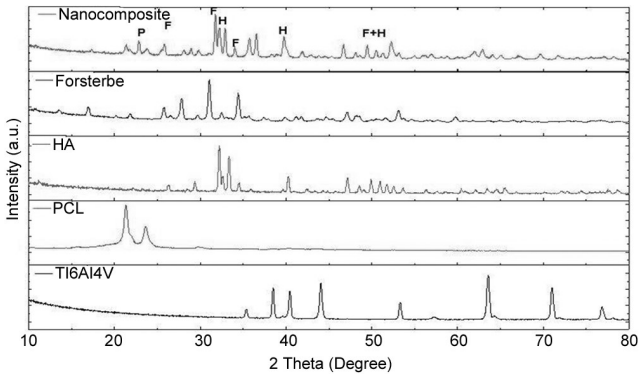

Fig. 4 — Stacked plot of different XRD patterns.

and 22.871 respectively. The peaks identified that the powder of forsterite was successfully synthesized[20]. Crystallite size of forsterite nanopowder was calculated by equation 1, which provided that the size was about 22.01 nm.

The X-ray diffraction of purchased hydroxyapatite nanopowder is shown in Fig. 3. The three strongest XRD peaks for HA powder were detected with Miller indices (121), (112) and (030), which corresponded to Bragg angles 31.8, 32.2 and 33.0 respectively. All peaks could be readily indexed to hexagonal HA structure with lattice constants a=b= 9.4120Å and c = 6.8950Å,calculated by using the unit cell method [21].

XRD pattern of composites

Figure 4 shows stackedXRD plots. The top most curve is shown for nanocomposite, where P,F and H denotes PCL, forsterite and hydroxyapatite. The bottom-most curve is shown for Ti6Al4V substrates. The curve matches with the standard curve for Ti6Al4V [22]. In the middle, the curves are shown for PCL, Hydroxyapatite and forsterite nanopowder, which matches with their standard ones. The nanocomposites curve showed combined peaks of PCL, hydroxyapatite, forsterite,and Ti6Al4V, which confirmed that thin film of nanocomposite (PCL-Forsterite-Hydroxyapatite)was successfully deposited over titanium substrate.

SEM analysis

SEM images of the coatings revealed that different morphologies were appeared due to forsterite and HA nanopowder content. The nanocomposite coatings were denoted as follows: Ti-4P-XF-YH, where X and Y is the percentage of forsterite and hydroxyapatite nanopowder in 4% fixed PCL matrix. SEM image of Ti-4P-2F-2H substrate showedthat addition of forsterite/HA nanoparticles into PCL producedthe thickand dense coating. In addition, no cracks were observed on the surface (Fig. 5a). The absence of cracks was considered good to protect the substrate from corroding and subsequently releasing metallic ions into the body fluids.

SEM image of Ti-4P-4F-4Hsubstrate showed that increase of forsterite/HA concentration resulted in the deposition of thicker, rougher and densely packed coating. The surface level pores were also observed with enhanced interfacial bonding (Fig. 5b); however, the coating was not very much denser than Ti-4P-2F-2H substrate. SEM image of Ti-4P-6F-6H substrate showed that nanoparticles were agglomerated on the surface, which led to the formation of surface level pores. This occurred due to ineffective interfacial bonding between nanoparticles, which corresponded to the reason that the PCL matrix was not enough to hold this high amount of HA/forsterite (Fig. 5c). The surface was having a high number of surface level pores, which were beneficial to promote osseointegration and diffusion of nutrients. SEM image of Ti-4P-8F-8H substrate indicated that cracks

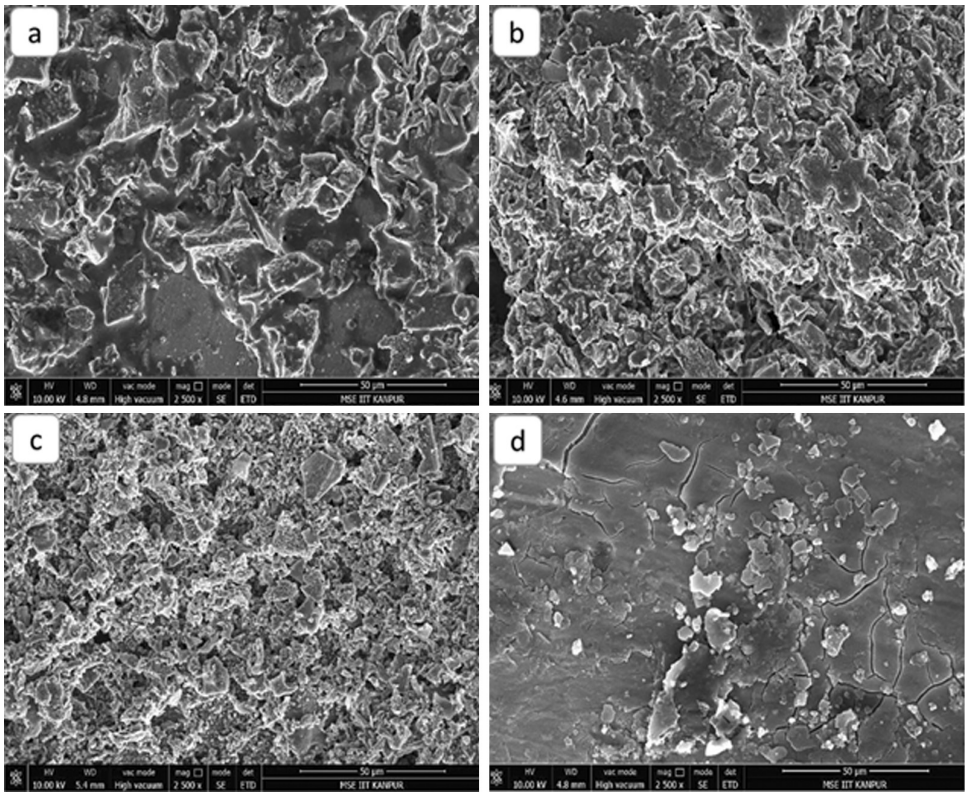

Fig. 5 — SEM images of (a) Ti-4P-2F-2H, (b) Ti-4P-4F-4H, (c) Ti-4P-6F-6H and(d) Ti-4P-8F-8H.

wered eveloped on the surface, which could accelerate the corrosion of metal surface.

Adhesion result

Since the execution of coatings specifically relied upon the mechanical trustworthiness of coating-substrate frameworks, the attachment of coatings to the substrates was evaluated to decide the strength and life span of the entire framework. Adhesion is a surface phenomenon, which is identified with the physical forces and chemical reactions at the coating-substrate interface. Different strategies have been applied to look at the adhesion strength of coatings. American Society of Testing and Materials (ASTM) test protocol D 3359 was utilized for finding the adhesion strength between PCL-HA-forsterite layers and the substrates, using adhesion test kit. This procedure comprised of applying and expelling pressure sensitive tape on the coating (more than 36 squares) and the assurance of the parts expelled from the surface during tests. Toward the finish of this test, the quantity of the parts expelled from the surface was estimated visually and the adhesion of coatings was appraised on the size of 0-5B. The scale‘5B’ alluded to the best coating strength and corresponded to the situation where the edges of the cuts were totally smooth and none of the squares of the grid was disconnected. The scale ‘0’ uncovered the most terrible strength amongst coating and substrates. The outcomes of the tests are shown in Table 1. It was evident from Table 1 that adhesion of coatings enhanced with an increase in forsterite and HA content in the PCL matrix. The parts of coating pilled from the surface of Ti-4P-8F-8H was 3 (classification 4B), which corresponded to the excellent coating adhesion with the substrate without any delamination and peeling; however, it was increased to 13 (classification 1B) in the case of Ti-4P-2F2H coated substrates, confirming very poor adhesion. Similarly,Ti-4P-4F-4H and Ti-4P-6F-6H showed classification 2B and 3B according to the parts of coating pilled from the surface. Significant improvement in adhesion with increasing forsterite and hydroxyapatite nanopowder content could be directly attributed to greater surface area and contact points, which were expected to enhance strength bonding between them.

Corrosion testing

The corrosion resistivity of uncoated and PCL/HA/Forsterite coated Ti6Al4V substrates was surveyed through potentiodynamic polarization and

Table 1 — Performance of coated Ti6Al4V substrates as per standard ASTM test

Substrate	Parts of coating pilled from the surface	Sample code
Ti-4P-2F-2H	13	1B
Ti-4P-4F-4H	10	2B
Ti-4P-6F-6H	6	3B
Ti-4P-8F-8H	3	4B

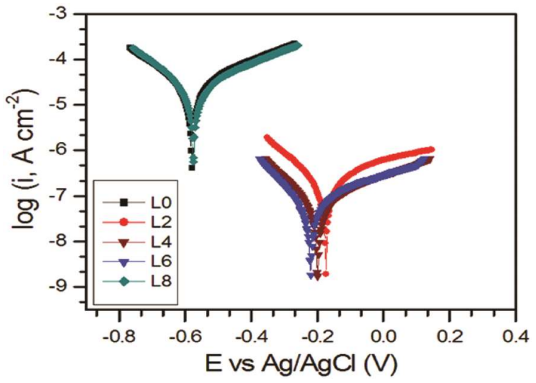

Fig. 6 — Plot of potential vs current density (Tafel polarization) of different substrates.

EIS analysis in PBS solution at room temperature. For transient corrosion reactions, Tafel curves and EIS curves were recorded after 30 min of immersion. Figure 6 presents Tafel polarization curves for Ti6Al4V substrates with different concentration of coatings. There are two parameters that are the most important in the study of corrosion protection: corrosion current density, I_{corr}; and equilibrium corrosion potential, E_{corr}. I_{corr} is responsible directly for corrosion performance and E_{corr} informs thermodynamic stability of the investigated system[23, 24].

Figure 6 revealed that I_{corr} was decreasing with the increase in F/HA content in the coating. Also, E_{corr} was shifting towards less negative potentials. Both the facts together portrayed that corrosion protection was greater with higher content of F/HA in the coatings[25]. However, Ti-4P-8F-8H substrate showed higher corrosion current than others, which meant that the coating was not enough able to protect the underneath substrate. This could happen due to cracks developed in the coating, through which acid could reach the base substrate. For detail discussion, the parameters are obtained by extrapolation of the curves and presented in Table 2.

From the analysis of Table 2, it was discovered that coated samples revealed less corrosion current density than uncoated Ti6Al4V, demonstrating enhanced

Table 2 — The analysis data extracted from potentio-dynamic polarization curves

Sample Names	Current density I_{corr}(A cm^{-2})	Potentials E_{corr} (V)	Efficiency η_{Rp}(%)
Ti6Al4V	2.18×10^{-5}	-0.59	-
Ti-4P-2F-2H	2.81×10^{-7}	-0.21	98.71
Ti-4P-4F-4H	6.76×10^{-8}	-0.22	99.68
Ti-4P-6F-6H	6.16×10^{-8}	-0.24	99.71
Ti-4P-8F-8H	1.99×10^{-5}	-0.57	8.71

corrosion resistance[26]. It could be due to the reduction of electron transfer provided by coatings. In addition, the incorporation of HA/Forsterite nanopowder resulted in shifting of the corrosion potential (E_{corr}) to more positive potential (Table 2). Moreover, the corrosion densities (I_{corr}) of the nanocomposite coated samples, (especially Ti-4P-6F-6H) were significantly reduced in comparison to uncoated Ti6Al4V. This fact confirmed that PCL-HA-forsterite coatings played a crucial role to improve the corrosion resistivity of Ti6Al4V. Even for Ti-4P-2F-2H, the protection efficiency was 98%. This fact suggested that less amount of the F/HA nanopowder in PCL matrix was also protective. The maximum efficiency was calculated as 99.71% for Ti-4P-6F-6H, which showed that 6% of F and HA nanopowder was the most effective for corrosion protection. In the case of Ti-4P-8F-8H, the corrosion current value was approximately the same as for Ti6Al4V, which corresponded to development of fine cracks in the coating due to the increase of HA/forsterite content in PCL solution. This incident increased the electron diffusion or electron work function (EWF) from PBS solution to the metal surface, which resulted in an increase of current density.

Figure 7 shows the results of the EIS test performed on coated and uncoated Ti6Al4V substrates. It was evident from Figure 7 that 2, 4 and 6 layers of PCL/HA/F coatings provided much more corrosion resistance in comparison to alone Ti6Al4V substrate. Figure 7 b is just a zoom view of Fig. 7a and is used to show the impedance of pure Ti6Al4V substrate. It was clear that the coated substrate had a much higher resistance than Ti6Al4V, which meant that corrosion of coated substrates was corroded at a much lower rate[27, 28]. Figure 7c shows Bode phase angle plots for uncoated and coated substrates, which revealed that the phase angle was higher than pure Ti6Al4V. This fact also indicated lower corrosion of coated substrates[29, 30]. The maximum corrosion resistance was offered by 6 layers PCL/F/HA coated Ti6Al4V substrate. The reason was that the coating

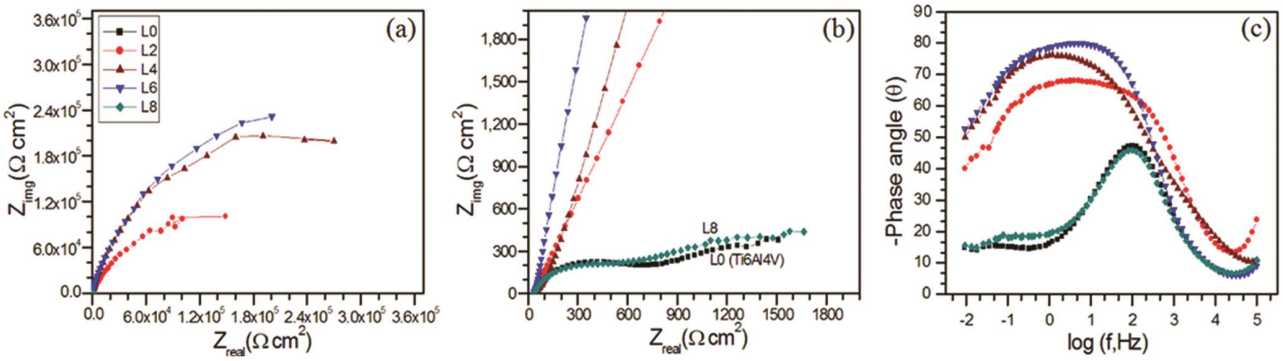

Fig. 7 — (a) Nyquist Plots of coated Ti6Al4V substrates; (b) zoom view of (a); (c) Bode phase angle plots for coated Ti6Al4V substrates.

covered the exposed area of reactive Ti6Al4V substrates and acted as a physical barrier for acid molecules. Due to the protective and compact nature of the coating, acid molecules could not penetrate into layers and less corrosion of the underneath substrate occurred. In contrast, the coating developed fine cracks on the surface in case of 8 layers of PCL/F/HA, which acted as a fined passage to acid molecules and allowed access to underneath substrate. That was why Ti-4P-8F-8H substrate showed similar corrosion resistance to uncoated Ti6Al4V.

Conclusion

Coatings of novel PCL-Forsterite-Hydroxyapatite nanocomposite were successfully deposited on Ti6Al4V substrates by dip coating and characterized for their microstructure, coating adhesion, roughness, and corrosion resistance. Results confirmed that a uniform, dense and crack-free layer of coatings were formed without any defect. Increase in forsterite and hydroxyapatite nanopowder significantly expanded the coating adhesion and roughness compared to the uncoated substrate. TPT and EIS results revealed that corrosion resistance of the nanocomposite coated substrates was much higher in comparison to uncoated substrates. The maximum corrosion resistance and protection efficiency were acknowledged for 6 layers PCL/F/HA coated Ti6Al4V substrate. Thus, our investigation projected that coating was protective in nature and amplified corrosion resistance of Ti6Al4V.

Acknowledgement

The authors are grateful to CIFC, IIT-BHU Varanasi and IIT Kanpur for providing research facilities.

References

1 Hanawa T, *Mater Sci Forum*, 512 (2006) 243.
2 Bache M & Evans W, *Int J Fatigue*, 23 (2001) 319.
3 Niinomi M, *J Mech Behav Biomed*, 1 (2008) 30.
4 Liu X, Chu P K & Ding C, *Mat Sci Eng R*, 47 (2004) 49.
5 Nouri A & Wen C, *Surface Coating and Modification of Metallic Biomaterials* (Woodhead Publishing,London), 2015, 3.
6 Adawy A &Fattah A, *Mat Sci Eng C-Mater*, 33 (2013) 1813.
7 Wang L & Li C, *Carbohyd Polym*, 68 (2007) 740.
8 Fihri A, Len C, Varma R S & Solhy A, *Coordin Chem Rev*, 347 (2017) 48.
9 Tadic D, Peters F & Epple M, *Biomaterials*, 23 (2002) 2553.
10 Holmes R, Bucholz R & Mooney V, *J Bone Joint Surg Am*, 68 (1986) 11.
11 Buchol R, Carlton A & Holmes R, *Clin Orthop Relat R*, 240 (1989) 5362.
12 Hench L L & Wilson J, *An Introduction to Bioceramics* (Imperial College Press, London), 1993, 229.
13 Saidi R, Fathi M H & Salimijaz H, *B Mater Sci*, 38 (2015) 1374.
14 Prakash P S, Pawar S J & Tewari R P, *P I Mech Eng L-J Mat*, (2017) .
15 Jokar M, Darvishi S, Torkaman R, KharazihaM & Karbasi M, *Surf Coat Tech,* 307 (2016) 324.
16 Yusoff M F, Kadir M R, Iqbal N, Hassan M A & Hussain R, *Surf Coat Tech*, 245 (2014) 102.
17 Mālnieks K, Mezinskis G, Pavlovska I, Bidermanis L & Pludons A, *Mater Sci-Medzg*, 21 (2015) 1320.
18 Singh M K, Gautam R K, Prakash R &Ji G, *Mechanical and corrosion behaviors of developed copper-basedmetal matrix composites* IOP Conf. Series: Materials Science and Engineering 330 (2018).
19 Ji G, Shukla SK, Dwivedi P, Sundaram S & Prakash R, *Ind Eng Chem* Res, 50 (2011) 11954.
20 Sanosh K P, Balakrishnan A, Francis L & Kim T N, *J Alloy Compd*, 435 (2010) 113.
21 Chandrasekar A, Sagadevan S & Dakshnamoorthy A, *Int J Phy Sci*, 8 (2013) 1639.
22 Prabhu M, Suriyaprabha R, RajendanV, Kulandaivelu P &Valiyaveettil, *RSC Adv*, 4 (2014) 43630.
23 JiG,Anjum S, Sundaram S & Prakash R, *Corros Sci*, 90 *(*2015) 107.
24 Ji G, Dwivedi P, Sundaram S & Prakash R, *Ind Eng Chem Res*, *52* (2013) 10673.
25 Ji G, Macıa LF, Allaert B, Hubin A & Terryn H, *J Electrochem Soc*, *165* (2018) 246.
26 Srivastava M, Tiwari P, Srivastava SK, Prakash R & Ji G, *J Mol Liq*, *236* (2017) 184.
27 Singh AK, JiG Prakash R, Ebenso EE & Singh AK, *Int J Electrochem Sci*, *8* (2013) 9442.
28 Tiwari P, Srivastava M, Mishra R,Ji G & Prakash R, *J Environ Chem Eng*, 6 (2018) 4773.
29 Singh AK, *Ind Eng Chem Res*, 51 (2012) 3215.